Received: 13 January 2023 | Revised: 30 March 2023 | Accepted: 24 May 2023

DOI: 10.1002/ccr3.7458

CASE REPORT

Clinical Case Reports Open Access WILEY

Histopathologic diagnosis of ultra-early autoimmune gastritis: A case report

Shuichi Terao[1] | **Shiho Suzuki**[1] | **Ryoji Kushima**[2]

[1]Department of Internal Medicine, Kakogawa Central City Hospital, Kakogawa, Japan

[2]Department of Pathology, Shiga University of Medical Science, Otsu, Japan

Correspondence
Shuichi Terao, Department of Internal Medicine, Kakogawa Central City Hospital, Kakogawa, Hyogo, Japan.
Email: stshiratodai2@gmail.com

Key Clinical Message

We describe an ultra-early stage of autoimmune gastritis (AIG) that occurs prior to the well-known early-stage AIG. The key pathology is the shortening of the second layer with degenerated parietal cells. In the management of patients with autoimmune diseases, AIG should be considered even if the endoscopy findings are normal.

KEYWORDS

autoimmune gastritis, endoscopic appearance, histological findings, shortening of the second layer, ultra-early

1 | INTRODUCTION

Autoimmune gastritis (AIG) was earlier known as gastritis characterized by advanced atrophy of fundic glands.[1] Thereafter, histopathologic studies gradually clarified the characteristics of early-stage AIG before advanced atrophy.[2–5] Recently, reports have introduced early-stage AIG cases with not only early-stage histological features, but also non-atrophic or slightly atrophic endoscopic images.[6–8] These reports are characterized by accompanying endoscopic findings that reflect other histological changes in the fundic gland, such as inflammation or hyperplasia. Additionally, one report[9] presented a case of early-stage AIG with a completely normal endoscopic appearance.

Herein, we report two cases with histological findings that are more subtle than those previously described; these may be termed "ultra-early-stage AIG."

2 | CASE REPORT

2.1 | Case 1

A 37-year-old woman with systemic lupus erythematosus and Sjögren's syndrome developed liver dysfunction in 2022 after 1 year of treatment. The patient underwent liver biopsy and was diagnosed with autoimmune hepatitis. Before starting prednisolone therapy, she underwent an upper gastrointestinal endoscopy. The patient had never received any acid secretion inhibitors, including proton pump inhibitors (PPIs) and vonoprazan.

On endoscopy, the antrum appeared normal (Figure 1A), and the gastric corpus exhibited normal coloration with a regular arrangement of collecting venules (RAC) (Figure 1C–E), which revealed normal round pit patterns on magnified narrow-band imaging (NBI) (Figure 1F). Additional findings included red streaks on

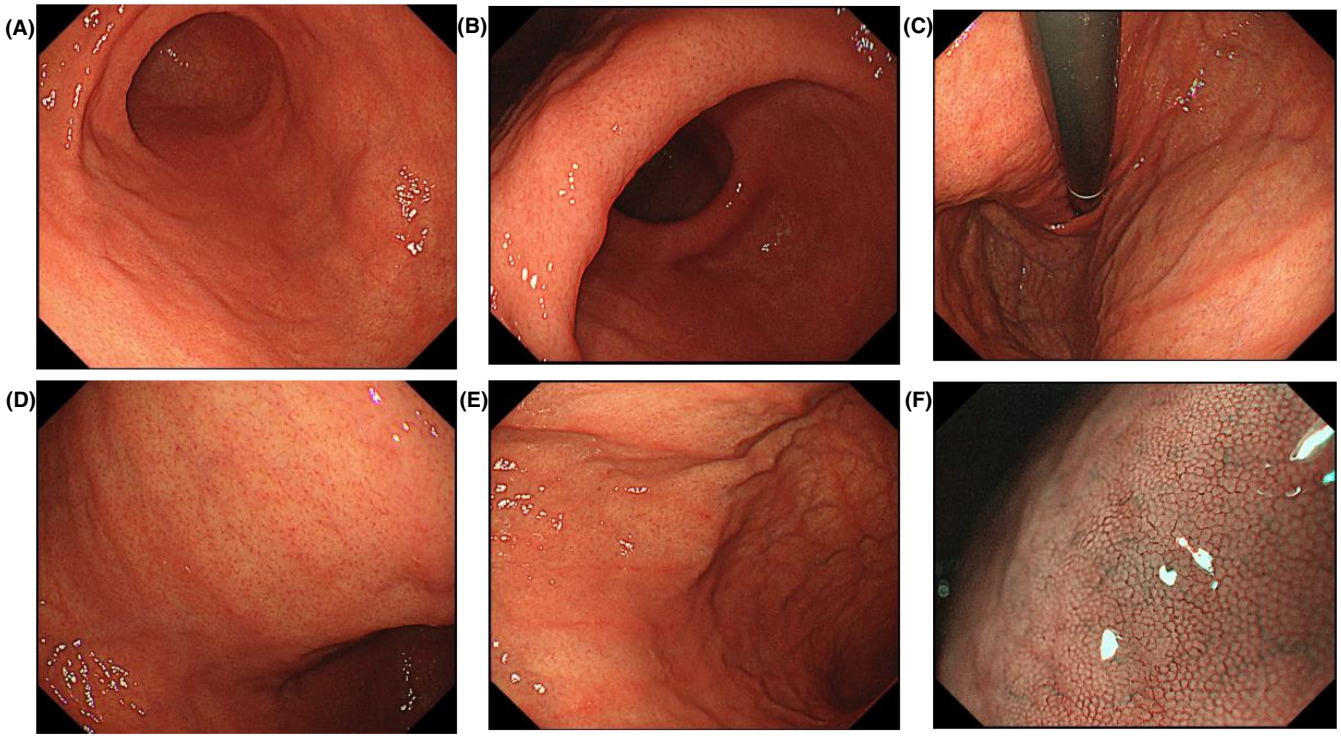

FIGURE 1 (A) Gastric antrum. (B) The lesser curvature of the angle. (C, D, E) Gastric corpus. (F) Magnified narrow-band imaging view of gastric corpus.

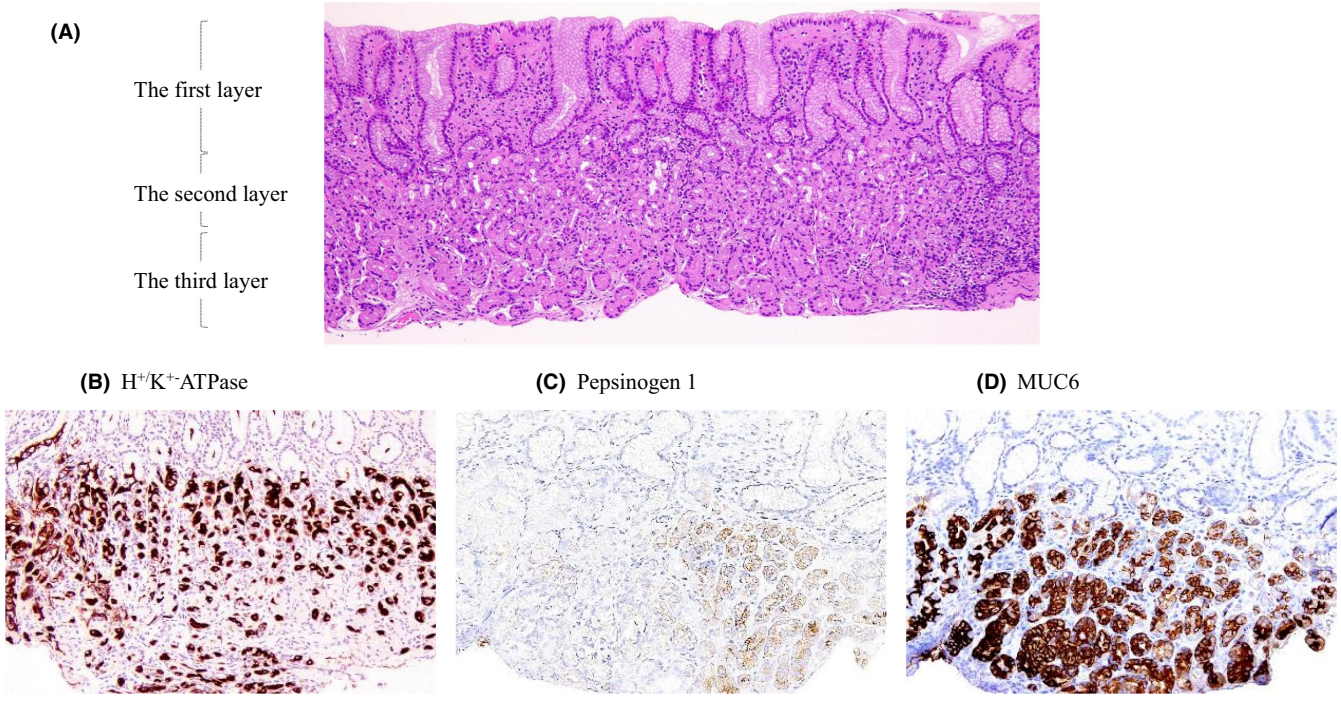

FIGURE 2 (A) Layer structure shown. (B) (C) (D) Comparison of different stainings in the same region of (A). (B) H+/K+-ATPase, (C) Pepsinogen 1, and (D) MUC6 staining (200x).

the corpus (Figure 1C,E) and slight mucosal swelling on the lesser curvature of the angle (Figure 1B).

Three biopsy specimens were taken from the greater curvature of the prepyloric area and the lesser and greater curvatures of the gastric corpus.

The histological findings of the prepyloric area revealed mild lymphocyte infiltration. Gastrin (G) secretory cells—revealed by gastrin-immunostaining—appeared to be mildly proliferated; however, an accurate assessment was difficult because the specimen was not cut vertically.

Three layers of the oxyntic mucosa were defined based on the distribution of cells observed upon hematoxylin and eosin (HE) staining, referring to figure 22.9 (page 603) from Histology for Pathologists by Mills[10]: the foveolae corresponded to the first layer, the pinkish parietal cells to the second layer, and the purplish chief cells to the third layer. In the lesser curvature of the middle corpus, the first layer (foveolar epithelium) presented as foveolar hyperplasia, the second layer (mainly parietal cells) showed shortening, and the third layer (mainly chief cells) was normally preserved in width. For all layers, the contours were slightly disorganized and the boundaries were slightly disrupted (Figure 2A). Parietal cells exhibited mild degeneration accompanied by moderate lymphocytic infiltration (Figure 2A). On additional immunostaining, $H^{+/}K^{+}$-ATPase stainability was heterogeneously reduced (Figure 2B), pepsinogen I (PG I) was negative in the left half and positive in the right half (Figure 2C), and MUC6 was positive throughout the region (Figure 2D). These findings indicated the coexistence of pyloric and pseudopyloric metaplasia. Chromogranin A staining showed the presence of slight enterochromaffin-like (ECL) cell hyperplasia. The boundaries of the three layers in the greater curvature of the middle corpus were destroyed and the first layer showed diffuse T-cell infiltration (Figure 3A,B) with CD3+, CD8+, and CD20- cells (Figure 3C–F).

The left column of Table 1 presents the laboratory data of the patient. The data obtained after endoscopy revealed that the anti-parietal cell antibody (PCA) titer was below 1:10 and anti-intrinsic factor antibody (IFA) was negative.

2.2 | Case 2

A 45-year-old woman was diagnosed with Hashimoto's disease (chronic thyroiditis), but had not received treatment because her condition had been stable for several years. She had not also been prescribed any drugs, including acid secretion inhibitors. The patient underwent a routine upper gastrointestinal endoscopy in 2022.

Endoscopy exhibited some minute discolored areas in the lesser curvature (Figure 4B) and the lower gastric corpus (Figure 4C). Although there were vascular visibilities on the antrum, corporeal, and fundic mucosa (Figure 4A,D,E), non-atrophic normal mucosal patterns were observed in the corporeal areas with a magnified

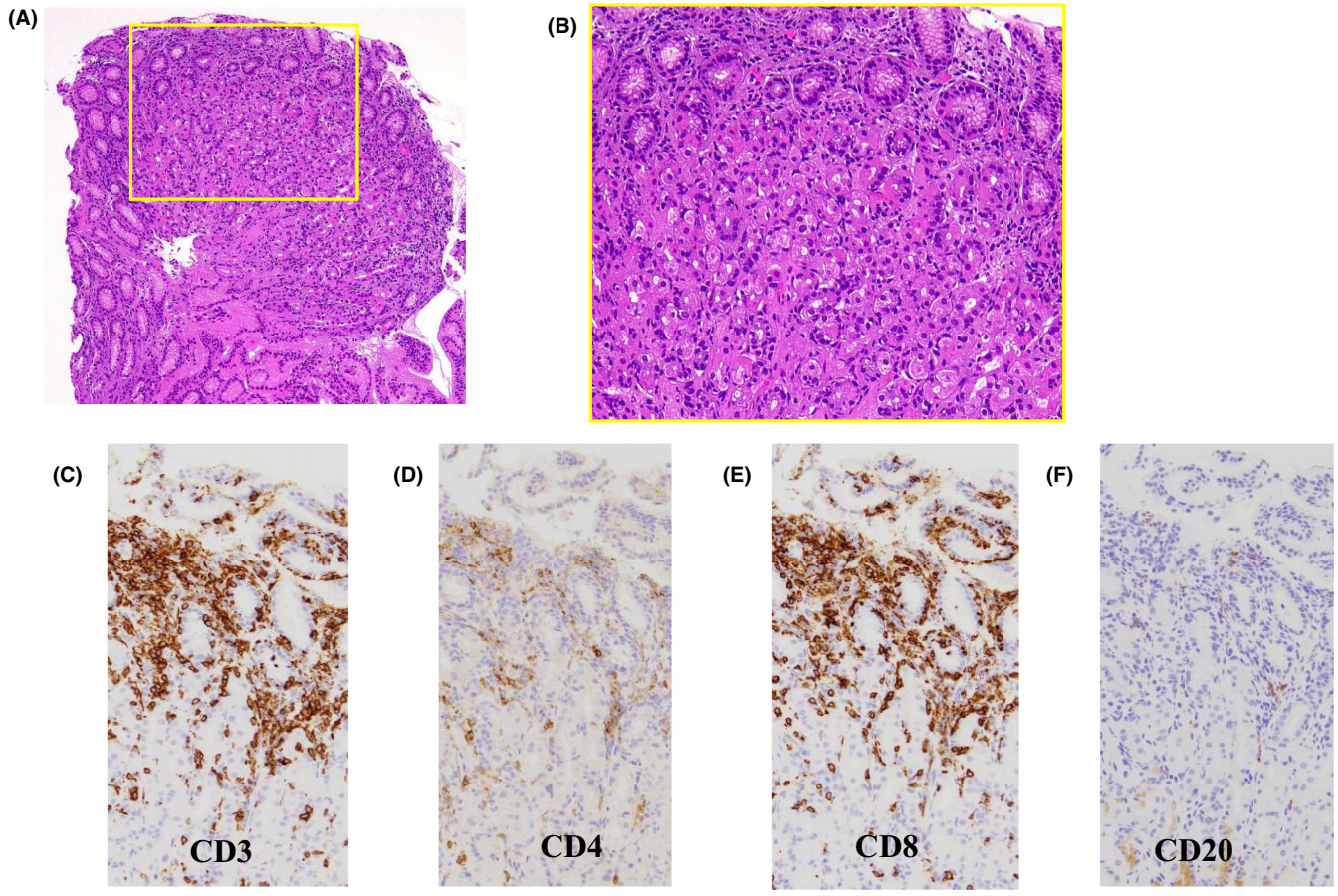

FIGURE 3 (A) Hematoxylin eosin (HE) staining (100x). (B) Hematoxylin eosin staining (200x) of the yellow-framed area in (A). (C) (D) (E) (F) CD3, CD4, CD8, and CD20 staining of the same region as (B).

TABLE 1 Laboratory findings of Case 1 and Case 2.

	Case 1	Case 2
Anti-parietal cell Ab. (<10)	<10	<10
Anti-intrinsic factor Ab. (−)	(−)	(−)
Gastrin (37~172 pg/mL)	150	75
Vit B12 (233~914 pg/mL)	870	540
Fe (40~188 μg/dL)	76	116
Anti-H. pylori IgG Ab. (<10 U/mL)	<3	<3
RBC (×10 000/μL)	381	393
Hb (11.6~14.8 g/dL)	11.4	12.5
MCV (83.6~98.2 fl)	91	93
TSH (0.50–5.00 μIU/mL)	2.25	2.54
FT4 (0.90–1.70 ng/dL)	1.05	0.69
Anti-TPO Ab. (<5.61 IU/mL)	n.a.	19.4
Antithyroglibulin Ab. (<4.11 IU/mL)	n.a.	519
Anti- nuclear Ab. (<40.0 IU/mL)	>2560	
Anti-ds-DNA Ab. (<12.0 IU/mL)	23.4	
Anti-SS-A/Ro Ab. (<10.0 U/mL)	>1200	
Anti-SS-B/La Ab. (<10.0 U/mL)	6.7	
Anti-RNP Ab. (<10)	>550	
AST (13~30 U/L))	291	
ALT (7~23 U/L)	376	
LD (124~222 U/L)	224	
ALP (38~113 U/L)	192	
IgG (861~1747 mg/dL)	3175	

Note: ( ) = normal range, unit.

Abbreviations: Ab, antibody; ALP, alkaline phosphatase level; ALT, alanine transaminase; AST, aspartate aminotransferase; ds-DNA, double-stranded deoxyribonucleic acid; Fe, iron; FT4, free thyroxine; H. pylori, Helicobacter pylori; Hb, hemoglobin; Ig, immunoglobulin; LD, lactate dehydrogenase; MCV, mean corpuscular volume; RBC, red blood cells; RNP, ribonucleoprotein; SS, Sjögren's-syndrome; TPO, thyroid peroxidase; TSH, thyroid stimulating hormone; Vit, vitamin.

NBI view (Figure 4F). Therefore, the vascular visibilities were judged to be unrelated to the histological glandular atrophy.

Three biopsy specimens were taken from the same sites as in Case 1. The prepyloric area demonstrated slight lymphocytic infiltration, but G cell hyperplasia was uncertain due to the specimen not being vertically cut for diagnosis. The only abnormality in the lesser curvature of the corpus was shortening of the second layer with slightly degenerated parietal cells. The first layer showed no hyperplastic change, and the third layer was normally preserved. The contour of the mucosal layer was also well-preserved with clearly recognized boundaries between the three layers (Figure 5). The greater curvature of the corpus showed a disorganized contour of the mucosal layer and exhibited mild hyperplastic change in the foveolar epithelium (Figure 6A). Parietal cells were mildly degenerated (Figure 6A,B), and PG I was positive (Figure 6C). MUC6 showed three staining patterns (Figure 6D): non-stained area, relatively uniformly stained area, and unevenly stained area. This difference was assumed to represent the progress of pseudopyloric metaplasia.

The laboratory data after endoscopy are presented in the right column of Table 1.

3 | DISCUSSION

3.1 | Histopathologic findings

Histological findings of the two cases are summarized in Table 2. We identified three phases in the process of early AIG:

First, the most minute histological changes (budding phase) were observed in the lesser curvature in Case 2. Lymphocytic infiltration was limited to focal areas, and the contour of the mucosal layer was completely preserved with clear layer boundaries. There was no foveolar hyperplasia, and the only structural change observed was the shortening of the second layer with slightly degenerated parietal cells (Figure 5). This minimal change is milder than previously reported for early-stage AIG.[2–4]

Second, slightly more advanced histological findings (intermediate phase) were found in the lesser curvature in Case 1 (Figure 2A) and greater curvature in Case 2 (Figure 6A). In these two sites, lymphocytic infiltration was mild or focal, and the contour of the mucosal layer was disorganized with slightly disrupted layer boundaries, but the layered structure was discernible. The second layer was relatively shortened, and the first layer showed foveolar hyperplasia.

Third, histological findings typical of conventional early-stage AIG were observed in the greater curvature in Case 1 (Figure 3A,B). Lymphocytic infiltration was diffuse, parietal cells were degenerated, and mild ECL cell hyperplasia was present. The layer boundaries were obscured, and the contour of the mucosal layer was completely destroyed. This phase was more advanced than the intermediate phase, with histological and endoscopic findings consistent with those in previously reported early-stage AIG.[2–4,6–8]

The shortened second layer in the budding phase is only recognizable when lymphocytic infiltration is minimal enough to preserve the contour of the three-layered structure. The rationale for considering minute changes alone to be indicative of early-stage AIG is that not only slight degeneration of parietal cells, but pseudopyloric and pyloric metaplasia of chief cells had already begun as exemplified in Figure 2B–D and Figure 6B–E. Additionally, the coexistence of two different phases in one individual, such as the conventional early and intermediate phases in Case 1 and the intermediate and budding phases in Case 2,

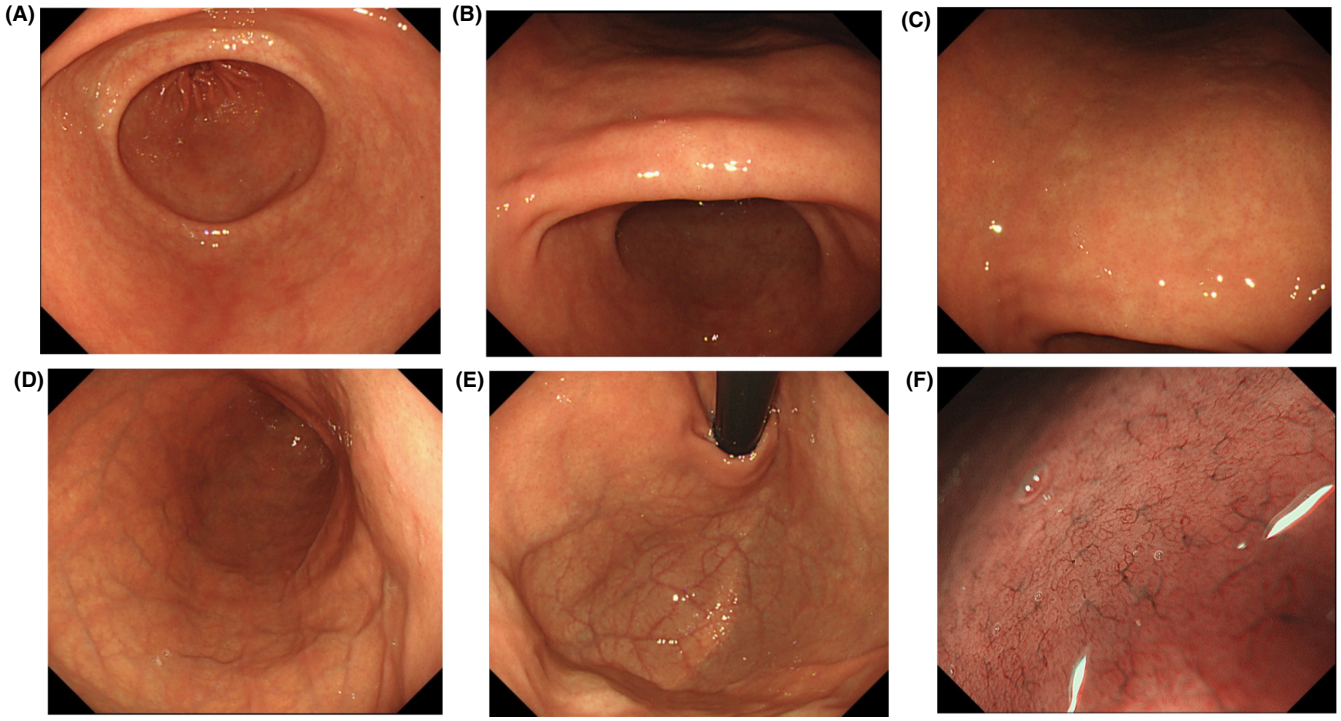

FIGURE 4 (A) Gastric antrum. (B) The lesser curvature of the angle. (C, D) Gastric corpus. (E) Gastric fundus. (F) Magnified narrow-band imaging view of gastric corpus.

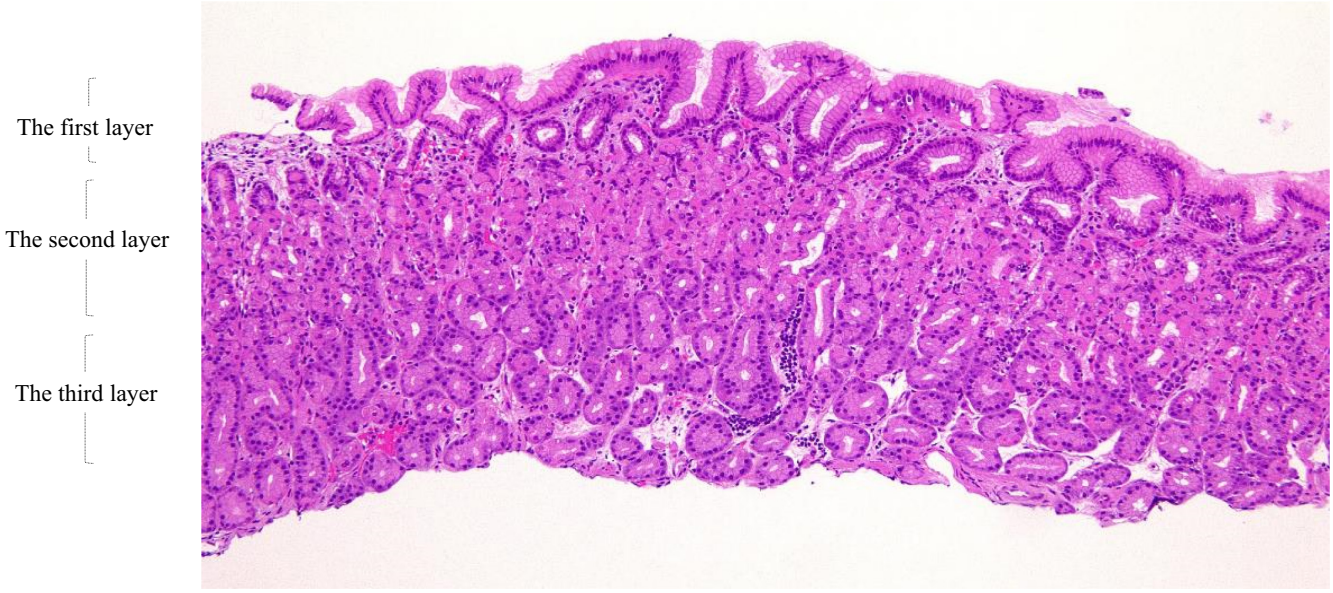

FIGURE 5 Histopathologic findings of the lesser curvature of corpus of Case 2.

indicates that early AIG progresses continuously from the budding, intermediate, and conventional early phases.

3.2 | Relationship with endoscopic findings

To evaluate the entire gastric mucosa, endoscopic findings should also be considered.

There were slight differences in endoscopic findings between the two cases. Case 1 showed red streaks and minimal mucosal swelling in the corpus, while Case 2 exhibited minute discolored areas in the lesser curvature of the corpus. However, both cases presented non-atrophic, nearly normal endoscopic appearances.

First, even in the endoscopically normal mucosa, histological changes representative of early-stage AIG had already begun. Second, histological differences

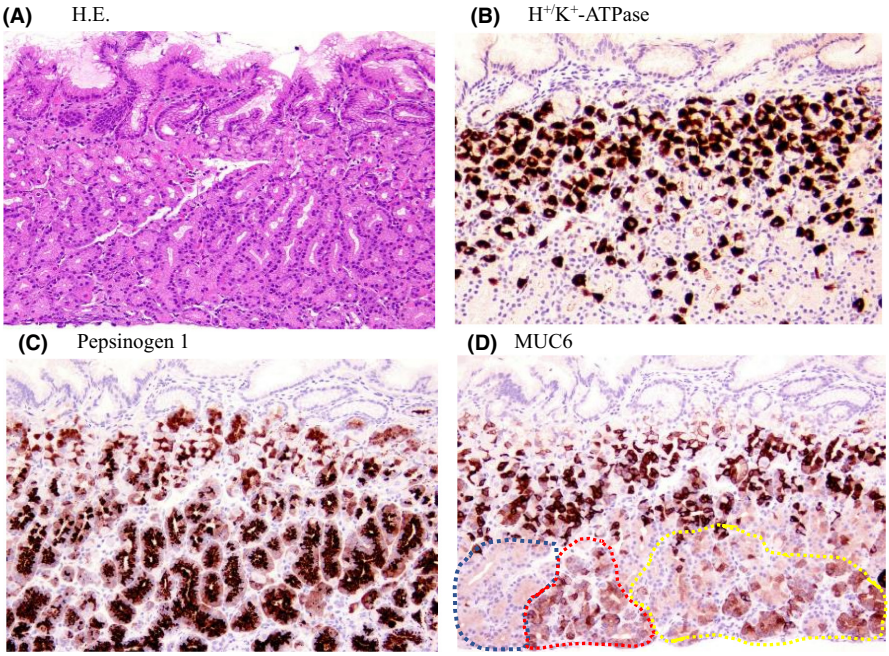

FIGURE 6 Comparison of different staining methods. (A) Hematoxylin eosin (HE), (B) H+/K+-ATPase, (C) Pepsinogen 1, and (D) MUC6 staining (200x). Blue-framed, non-stained area; red-framed, relatively uniformly stained area; yellow-framed, unevenly stained area.

TABLE 2 Histological comparison between Case 1 and Case 2.

			Case 1	Case 2
Antrum				
	Lymphocyte infiltration		Mild	Slight
	Gastrin cells		Mild hyperplasia	Mild hyperplasia
	Atrophy		None	None
Lesser curvature of the corpus				
	Contour of the mucosal layer		Slightly disorganized	Preserved
		The first layer	Lengthened	Normal
		The second layer	Shortened	Shortened
		The third layer	Normal	Normal
		Layer boundaries	Slightly disrupted	Clear
	Parietal cell		Mildly degenerated	Slightly degenerated
	Lymphocyte infiltration		Mild	Focal, slight
	Atrophy		None	None
	Metaplasia		Pyloric and pseudopyloric	Pyloric and pseudopyloric
	ECL cell hyperplasia		Slightly positive	None
Greater curvature of the corpus				
	Contour of the mucosal layer		Destroyed	Disorganized
		The first layer	Indistinguishable	Lengthened
		The second layer	Indistinguishable	Shortened, collapsed
		The third layer	Indistinguishable	Normal
		Layer boundaries	Obscured	Disrupted
	Parietal cells		Degenerated	Degenerated
	Lymphocyte infiltration		Diffuse	Focal, slight
	Atrophy		None	None
	Metaplasia		Pyloric and pseudopyloric	Pyloric and pseudopyloric
	ECL cell hyperplasia		Slightly positive	None
	Description of background fill			
		Conventional early phase		
		Intermediate phase		
		Budding phase		
ECL, enterochromaffin-like				

in progression representative of early-stage AIG were detected even in the mucosa assessed as normal on endoscopy.

Recently, a case of early-stage AIG was reported with a normal endoscopic appearance.[9] However, in this report, despite milder lymphocyte infiltration in the lesser curvature of the gastric corpus compared to the greater curvature (where lymphocyte infiltration was dense), the contour of the mucosal layer was disorganized with obscured layer boundaries even in the lesser curvature.

As these abnormalities depend on the degree of lymphocyte infiltration, our cases (the lesser and lesser and greater curvatures of Cases 1 and 2, respectively) showed ultra-early-stage AIG characteristics.

3.3 | Clinical manifestations

Both cases were negative for autoantibodies (PCA, IFA), which are generally assumed to be the basis for the diagnosis of AIG. PCA is sensitive for AIG and the PCA-positive rate in AIG patients is approximately 85–90%; however, it is not specific for AIG because PCA-positivity is observed in conditions such as *H. pylori* infection and other autoimmune diseases.[11] Additionally, some experimental reports in a thymectomized Balb/c mouse model suggest that mucosal damage in AIG is caused by H^+/K^+-ATPase-specific cytotoxic T-cells,[12] and PCA is generated in the process of parietal cell injury.[13] Thus, PCA is not considered a cause of AIG[14]; this means the PCA-negativity in the two cases described herein, in which tissue damage was minimal, is not a basis for not diagnosing AIG.

IFA positivity is also not required for AIG, with a positivity rate of approximately 60%[15] and a greater likelihood of positivity in the late stages of AIG.[16]

Serum gastrin levels were within normal ranges in both cases. Serum gastrin increases with the progression of AIG,[17] but its levels in early AIG are unknown. Hypergastrinemia did not occur as acid secretion was probably not yet suppressed.

H. pylori (Hp)-IgG antibody was negative in both cases. Endoscopy was consistent, and the histological findings did not demonstrate Hp-infected gastritis, indicating these were Hp-uninfected cases.

The absence of anemia in both cases does not contradict the AIG diagnosis. The frequency of iron deficiency anemia in AIG is not very high, as reported in Italy (27%)[18] and Japan (6.5%).[19] Vitamin B_{12} deficiency anemia has approximately 24.6%[20] incidence in AIG patients, but it is rare in younger patients.[21]

Both patients had other autoimmune diseases and were positive for various autoantibodies, which were clues to identifying early-stage AIG. We plan to follow-up both the patients at 1-year post diagnosis and measure PCA and/or IFA and evaluate their progress to overt AIG.

Based on these considerations, we concluded that "shortening confined to the second layer" is a characteristic finding of ultra-early-stage AIG and represents the onset of early-stage AIG.

3.4 | Differential diagnosis

Two points should be noted in the differential diagnosis. First, PPI or vonoprazan use must be verified. These drugs induce degeneration of parietal cells, which may be histologically confusing with our cases. Second, it is important to note that parietal cell dysfunction also shows changes confined to the second layer, but its histology is quite different. Parietal cell dysfunction is characterized by the thickening of the second layer with vacuolated degeneration of the parietal cells,[22] which is quite the opposite of the findings in the lesser curvature of the middle corpus in Cases 1 and 2.

In conclusion, we herein present an ultra-early-stage of AIG—a stage that occurs prior to the previously reported early-stage. The key finding is "shortening confined to the second layer". Understanding the broad spectrum of AIG will facilitate early detection and better control of its complications.

AUTHOR CONTRIBUTIONS

Shuichi Terao: Conceptualization; data curation; investigation; supervision; visualization; writing – original draft. **Shiho Suzuki:** Conceptualization; data curation; investigation. **Ryoji Kushima:** Conceptualization; investigation; supervision.

FUNDING INFORMATION

This study received no external funding.

CONFLICT OF INTEREST STATEMENT

The authors have no conflict of interest to declare.

DATA AVAILABILITY STATEMENT

The data that support the findings of this study are available on request from the corresponding author. The data are not publicly available due to ethical restrictions.

ETHICS STATEMENT

All procedures were performed in accordance with the ethical standards of the Declaration of Helsinki (1964) and its later amendments. This study was approved by the clinical research ethics review committee of Kakogwa Central City Hospital on February 12, 2021 (approval number: 28-12).

PATIENT CONSENT

Written informed consent was obtained from the two patients in this study.

ORCID

Shuichi Terao https://orcid.org/0000-0003-4234-0524

REFERENCES

1. Strickland RG, Mackay IR. A reappraisal of the nature and significance of chronic atrophic gastritis. *Am J Dig Dis*. 1973;18:426-440.
2. Stolte M, Baumann K, Bethke B, Ritter M, Lauer E, Eidt H. Active autoimmune gastritis without total atrophy of the glands. *Z Gastroenterol*. 1992;30:729-735.
3. Torbenson M, Abraham SC, Boitnott J, Yardley JH, Wu TT. Autoimmune gastritis: distinct histological and immunohistochemical findings before complete loss of oxyntic glands. *Mod Pathol*. 2002;15:102-109.
4. Greenson JK, Lauwers GY, Montgomery EA, et al., eds. *Diagnostic Pathology: Gastrointestinal*. 3rd ed. Elsevier; 2019:140-143.
5. Takemura S, Nakajima S, Wada Y, et al. [pathological diagnosis of autoimmune gastritis] Jikomen-eki sei ien no byouri shindan (in Japanese). *Byouri to Rinsho (Pathology and Clinical Medicine)*. 2021;39:537-544.
6. Kotera T, Oe K, Kushima R, Haruma K. Multiple pseudopolyps presenting as reddish nodules are a characteristic endoscopic finding in patients with early-stage autoimmune gastritis. *Intern Med*. 2020;59:2995-3000.
7. Ayaki M, Aoki R, Matsunaga T, et al. Endoscopic and upper gastrointestinal barium X-ray radiography images of early-stage autoimmune gastritis: a report of two cases. *Intern Med*. 2021;60:1691-1696.
8. Kishino M, Yao K, Hashimoto H, et al. A case of early autoimmune gastritis with characteristic endoscopic findings. *Clin J Gastroenterol*. 2021;14:718-724.
9. Kotera T, Yamanishi M, Kushima R, Haruma K. Early autoimmune gastritis presenting with a normal endoscopic appearance. *Clin J Gastroenterol*. 2022;15:547-552.
10. Mills SR. *Histology for Pathologists*. 5th ed. Wolters Kluwer; 2019:605-606.
11. Rustgi SD, Bijlani P, Shah SC. Autoimmune gastritis, with or without pernicious anemia: epidemiology, risk factors, and clinical management. *Therap Adv Gastroenterol*. 2021;14:17562848211038771.
12. Nishio A, Hosono M, Watanabe Y, Sakai M, Okuma M, Masuda T. A conserved epitope on H+, K+ adenosinetriphosphatase of parietal cells discerned by a murine gastritogenic T-cell clone. *Castroenterol*. 1994;107:1408-1414.
13. Kojima A, Taguchi O, Nishizuka Y. Experimental production of possible autoimmune gastritis followed by macrocytic anemia in athymic nude mice. *Lab Invest*. 1980;42:387-395.
14. Toh BH, van Driel IR, Gleeson PA. Pernicious anemia. *N Engl J Med*. 1997;337:1441-1448.
15. Tozzoli R, Kodermaz G, Perosa AR, et al. Autoantibodies to parietal cells as predictors of atrophic body gastritis: a five-year prospective study in patients with autoimmune thyroid diseases. *Autoimmun Rev*. 2010;10:80-83.
16. Lahner E, Norman GL, Severi C, et al. Reassessment of intrinsic factor and parietal cell autoantibodies in atrophic gastritis with respect to cobalamin deficiency. *Am J Gastroenterol*. 2009;104:2071-2079.
17. Miceli E, Vanoli A, Lenti MV, et al. Natural history of autoimmune atrophic gastritis: a prospective, single Centre, long-term experience. *Aliment Pharmacol Ther*. 2019;50:1172-1180.
18. Annibale B, Capurso G, Chistolini A, et al. Gastrointestinal causes of refractory iron deficiency anemia in patients without gastrointestinal symptoms. *Am J Med*. 2001;111:439-445.
19. Terao S, Suzuki S, Yaita H, et al. Multicenter study of autoimmune gastritis in Japan: clinical and endoscopic characteristics. *Dig Endosc*. 2020;32:364-372.
20. Villanacci V, Casella G, Lanzarotto F, et al. Autoimmune gastritis: relationships with anemia and helicobacter pylori status. *Scand J Gastroenterol*. 2017;52:674-677.
21. Bizzaro N, Antico A. Diagnosis and classification of pernicious anemia. *Autoimmun Rev*. 2014;13:565-568.
22. Abe Y, Hatta W, Asonuma S, et al. Parietal cell dysfunction: a rare cause of gastric neuroendocrine neoplasm with achlorhydria and extreme Hypergastrinemia. *Intern Med*. 2022;61:2441-2448.

How to cite this article: Terao S, Suzuki S, Kushima R. Histopathologic diagnosis of ultra-early autoimmune gastritis: A case report. *Clin Case Rep*. 2023;11:e7458. doi:10.1002/ccr3.7458